Available online at www.sciencedirect.com

SCIENCE DIRECT®

Ecological Modelling 177 (2004) 157–177

ECOLOGICAL MODELLING

www.elsevier.com/locate/ecolmodel

Predicting juvenile salmonid drift-feeding habitat quality using a three-dimensional hydraulic-bioenergetic model

D.J. Booker[a,*], M.J. Dunbar[a], A. Ibbotson[b]

[a] *Centre for Ecology and Hydrology, Maclean Building, Crowmarsh Gifford, Wallingford, Oxon OX10 8BB, UK*
[b] *Centre for Ecology and Hydrology, Winfrith Technology Centre, Dorchester, Dorset DT2 8ZD, UK*

Received 14 May 2003; received in revised form 23 December 2003; accepted 5 February 2004

Abstract

This paper describes a physically based three-dimensional bioenergetic model for prediction of physical habitat quality for drift-feeding juvenile salmonids in a river. A three-dimensional Computational Fluid Dynamics (3D-CFD) model is used to simulate hydraulic patterns in a 50 m reach of the Bere stream, Dorset, UK. This information is then combined with a bioenergetic model that uses behavioural and physiological relationships to quantify the spatial pattern of energy gain when drift feeding. The model was tested by comparing patterns of predicted energy intake with observed habitat use by juvenile salmonids at different times of day.

Hydraulic measurements or predictions are required as input to bioenergetic models to calculate the foraging range of the fish. Horizontal and vertical velocity gradients can be high and variable in shallow streams with complex topography and roughness zones. In this paper, a three-dimensional hydraulic model enables more realistic calculation of the foraging area of the fish. This takes account of the complexity of horizontal and vertical velocity gradients. Numerical experiments are used to demonstrate the sensitivity of energetic gain to changes in the method of calculating foraging area. Results support the hypothesis that feeding fish preferentially select areas of high energy gain, but move to areas of lower velocity when resting.

Keywords: Bioenergetic modelling; Computational Fluid Dynamics; Drift feeding; Atlantic salmon; Brown trout; Hydraulic modelling; Foraging model

1. Introduction

Assessment of physical habitat in rivers is often used as a method for determining the impacts of management, such as flow regulation (Acreman et al., 2000) or river restoration (Maddock, 1999), on communities and species of interest. Most commonly, physical habitat modelling has made use of pseudo two-dimensional, empirically based models, such as PHABSIM (PHysical HABitat SIMulation) (e.g. Bovee, 1982; Elliott et al., 1999). This approach uses modelled distributions of depth, velocity and substrate to define areas of useable physical habitat. Modelling physical habitat allows assessment of habitat conditions beyond their measured range. However, these approaches may be criticised for including hydraulic modelling approaches that are not physically based (Booker, 2003), employing Habitat Suitability Indices (HSIs) that are often not fully tested (Gore and Nestler, 1988) and relying on at-a-point assessments of physical habitat that are not spatially related (Crowder and Diplas, 2000a).

* Corresponding author. Tel.: +44-491-692356.
E-mail address: dobo@ceh.ac.uk (D.J. Booker).

0304-3800/$ – see front matter © 2004 Elsevier B.V. All rights reserved.
doi:10.1016/j.ecolmodel.2004.02.006

The spatial distribution of physical habitat conditions in rivers is a function of hydraulic, sedimentary, morphological and cover conditions (e.g. Binns and Eiserman, 1979; Jungwirth, 1988; Parasiewicz and Dunbar, 2001). Organisms, such as fish, make use of this template for different activities and life stages (Shirvell and Dungey, 1983; Heggenes and Saltveit, 1990). Development of habitat modelling approaches that capture the spatial distribution of habitat are necessary for understanding of ecological processes. Further, many management options involve changes to a system that go beyond the experience of natural conditions and this requires the development of numerical modelling tools.

A great deal of research has been conducted into feeding (e.g. Wankowski, 1979), habitat use (e.g. Armstrong et al., 2003), spawning (e.g. Soulsby et al., 2001; Volpe et al., 2001) and physiology (e.g. Lin et al., 2003) of salmonids in freshwater. However, assessment of juvenile salmonid habitat quality to support water management decisions remains difficult. Heggenes (1996) stated that unless dynamic aspects of habitat selection are incorporated into the habitat models the long-term predictive utility of habitat-hydraulic modelling is limited. An alternative to describing habitat use by empirical functions is to explain habitat use and growth by quantifying the balance between energy gained through feeding and energy lost through swimming, digestion, food capture, growth, reproduction, urine and faeces (Fausch, 1984). Such an energetic approach can be physically based by including the environmental factors that influence fish survival and growth (Hayes et al., 2000). This has the advantage of providing spatially continuous patterns of habitat necessary for creating individual-based models (IBMs) (Grimm, 1999; Scheibe and Richmond, 2002) of fish life histories and populations. Physically based approaches also provide the predictive capability necessary to inform managers of the potential effects of future changes in the environment, such as those caused by climate changes or water abstraction.

Bioenergetic models have been developed for prediction of microhabitat use (e.g. Hughes and Dill, 1990; Hughes, 1992; Hill and Grossman, 1993; Guensch et al., 2001) and long-term growth (Clark and Rose, 1997; Railsback and Rose, 1999; Hayes et al., 2000) for salmon and trout in rivers. However, most of this research has relied on field measurement or hypothetical hydraulic input, prohibiting spatially continuous calculations. One exception is Hayes et al. (2003) who utilised two-dimensional hydraulic model predictions as input to a drift dispersion model and a bioenergetic drift-feeding model. The most important factors in the bioenergetic balance of drift-feeding fish are temperature, food supply, swimming activity and the hydraulics acting upon the fish. Information relating to the spatial and temporal variations in these variables could be gained from field measurements alone. However, repeated measurement would be expensive and lack the predictive capability required for water resource assessment and the spatial and temporal information required for IBMs.

Following field-based approaches, models of juvenile salmonid habitat quality have traditionally been based on measurements recorded at locations where fish have been found (e.g. Beecher et al., 2002). However, juvenile salmonids drift feed over an area across which hydraulic conditions may vary. It is logical that habitat quality should not just be defined by conditions at the location where the fish is found, but also by those surrounding the fish. Coupling of spatial hydraulic and bioenergetic models therefore allows a spatial assessment of energy gain for drift-feeding fish. This can be compared with measured locations of fish to test whether fish select areas of river with high predicted energy gain.

This paper describes the formulation and testing of a physically based bioenergetic model that can be used to predict energy gain for juvenile salmonids. The aim of the work is to demonstrate that knowledge of the processes controlling hydraulics and physiology can be combined in order to produce testable physically based habitat predictions.

2. Methods

2.1. Field methodology

The study reach was a 50 m length of the Bere stream, Dorset, UK, approximately 1 km upstream of its confluence with the River Piddle (NGR SY859922). The reach of interest contained glides, riffles and pools. Substrate was predominantly fine gravel in the size range of 2–64 mm although some

discrete areas of sand and silt were present. There was no vegetation rooted to the river bed although tree branches were present in the channel. The channel was approximately 5 m wide.

Juvenile trout and salmon were located by direct observation by upstream snorkel diving. The entire river bed was searched for fish. Each fish was observed for 2 min. If the fish was actively searching the water column or intercepting drift it was recorded as feeding. Other fish that appeared to be static or not searching the water column were recorded as resting. The location of the fish, its length, species and activ-

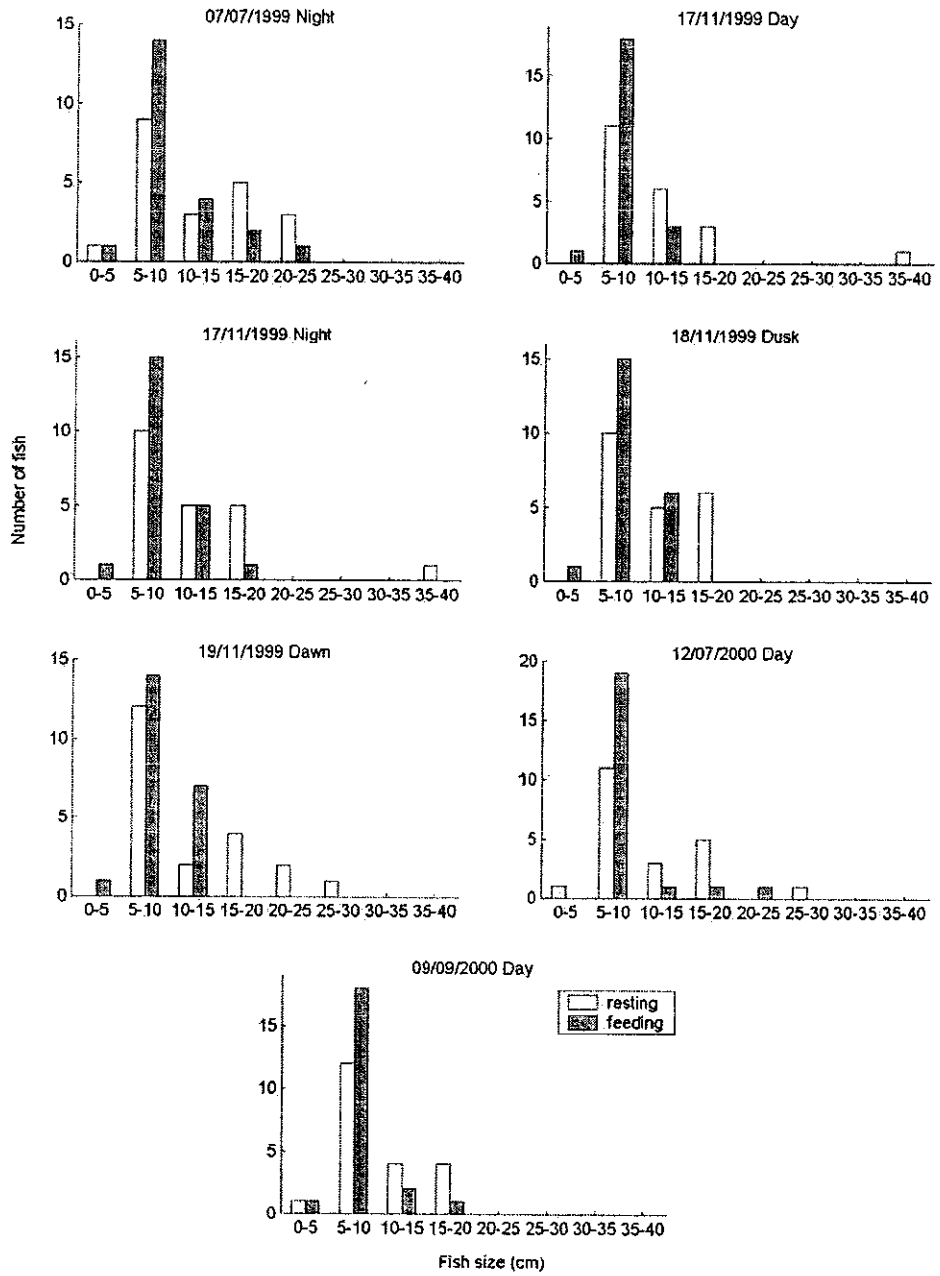

Fig. 1. Histogram of fish sizes observed on each occasion (white bars: resting, gray bars: feeding).

ity were recorded (Fig. 1). The positions of all fish were recorded using a Zeiss Elta total station. This procedure was repeated on six occasions (Table 1). Permanent survey markers were used to ensure all measurements were made to a consistent site datum. The six occasions were at different times of the year and time of day.

Invertebrate drift was sampled to provide input to the bioenergetic model. Drift was sampled during each fish observation occasion, at a single location in the deepest part of a glide 50 m upstream of the reach where fish were observed. A single net with a square mouth of 1 m × 1 m and 1 mm mesh size was placed in the centre of the channel with one side flush with the river bed, and the opposite side above the water surface (Elliott, 1970). Sampling occurred for the entire time that the fish were observed. Water velocity at the mouth of the net was measured using a Valeport 801 electromagnetic current meter to estimate volume of water sampled. Macroinvertebrates were counted, identified to family level and their length measured. The majority of the taxa were Ephemeroptera (39%), Crustacea (*Gammarus pulex*) (31%), terrestrial insects (13%) and Diptera (8%). For each size class denoted in Table 1 the density was calculated according to

$$n_{\text{density}} = \frac{n_{\text{obs}}}{vAt_{\text{obs}}} \quad (1)$$

where the number of prey in each cubic meter of water is n_{density}, n_{obs} is the number of prey caught, A is the net area, t_{obs} is the total measurement time and v is the velocity at the net.

A Campbell CR10 logger was installed at the site, allowing continuous measurement of water temperature, stage (through a pressure transducer), light (in terms of solar energy) on the bank, turbidity and pH. Measurements were taken every 10 s, averaged and logged hourly.

2.2. Hydraulic simulation methodology

The SSIIM Computational Fluid Dynamics (CFD) model was used to simulate patterns of hydraulics for this investigation (Olsen, 1996, 2000). The model uses a finite difference approach to solve the three-dimensional Navier–Stokes equations, with a two-equation k-ε turbulence closure model (Olsen and Stokseth, 1995; Booker et al., 2001; Harby and Alfredsen, 1998; Booker, 2003).

Table 1
Measured conditions, fish activities and drift densities

Snorkelling conditions								Fish activities (number of fish)			n_{density} (animals per m^3)							
											Prey sizes (mm)							
Date	Time of day	Time (h)	Discharge (ms^{-3})	Stage above datum (m)	Solar energy, bank (W m^{-2})	Temperature (°C)	Feeding	Resting	Total	0–4.9	5–7.9	8–9.9	10–11.9	12–14.9	15–19.9	20–30
07/07/1999	Night	01:00	0.41	9.663	0	15	12	18	30	0.378	1.058	1.058	0.12	0.054	0.006	0.003
17/11/1999	Day	13:00	0.40	9.670	211.7	8.9	20	25	45	0.002	0.006	0.002	0.002	0.002	0	0
17/11/1999	Night	00:00	0.40	9.665	0	6.1	5	27	32	0.013	0.01	0.023	0.02	0.002	0.003	0
18/11/1999	Dusk	17:00	0.40	9.664	0.165	7.9	8	39	47	0.006	0.014	0.014	0.009	0.005	0	0
12/07/2000	Day	12:00	0.44	9.690	248.3	14.2	42	40	82	0.241	0.02	0.001	0	0	0	0
09/09/2000	Day	11:00	0.36	9.580	166.3	13.6	38	10	48	0.206	0.06	0	0	0	0	0
Average summer n_{density}										3.101	0.686	0.171	0.047	0.029	0.021	0.032

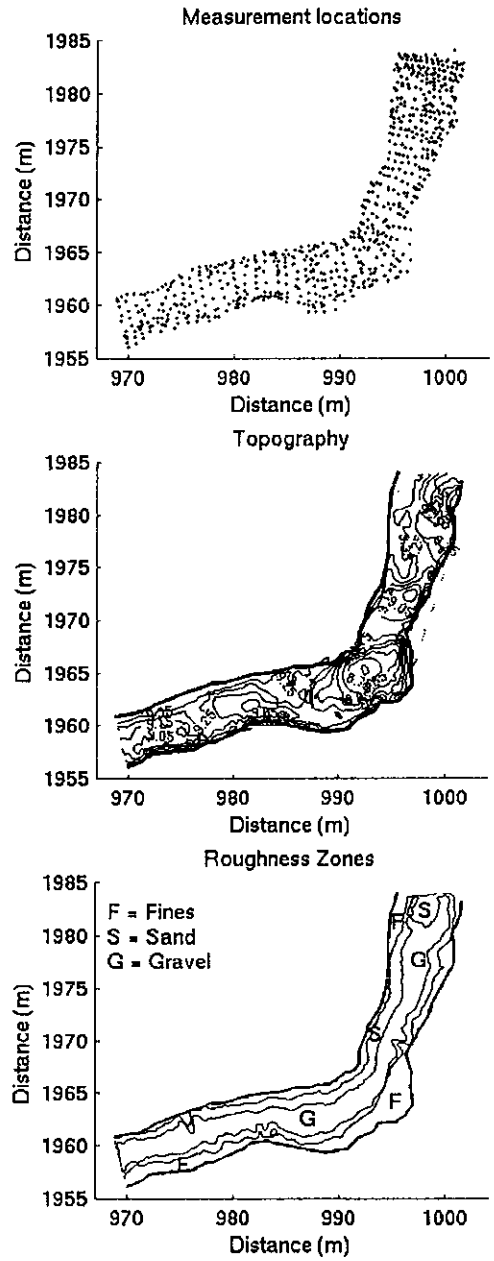

Fig. 2. Topography measurements, roughness zones, the numerical grid and the topography at the site.

A total of 835 topography points were measured at the site using a Zeiss Elta total station (Fig. 2). The approximate point density of these measurements equates to a measurement every 0.31 m^2. A numerical grid required to run the model was then created from these topography data. The positions of tree branches on the river bed were also measured using the total station and, where possible, were included in the topography data set. The numerical grid was a $287 \times 40 \times 7$ matrix of 80,360 cells. The dimensions of each cell were approximately 0.15 m × 0.12 m × 0.10 m. Rules for grid quality outlined by Bernard (1993) and repeated by Lane et al. (1999) were followed in grid design.

Table 2
Roughness sizes set for each roughness zone

Zone	Roughness height, k_s (m)	Multiplier	Sediment size, D_{84} (m)
Fines	0.0105	3.5	0.003
Sand	0.021	3.5	0.006
Gravel	0.105	3.5	0.03
Banks	0.400	n/a	n/a

Distinct zones of fine silt, sand and gravel were present at the site. The locations of these zones were surveyed in the field and used to set the spatial distribution of k_s (roughness height) in the model (Fig. 2 and Table 2). Roughness height parameters were set based on $3.5D_{84}$ (cf. Hey, 1986; Clifford et al., 1992). This method of roughness characterisation takes account of particles larger than the median having a greater influence on flow resistance (Leopold et al., 1964). Table 2 shows the sediment sizes for D_{84} of each sediment type and the k_s values used for each zone. Bank roughness was set to 0.4 m to reflect the strong roughness effects of twigs and branches along the banks. This high value of bank roughness corresponded well with measurements of slow near-bank velocity. At the upstream boundary a uniform cross-stream velocity pattern was imposed, with vertically varying downstream velocity defined by the logarithmic profile, and zero cross-stream and vertical velocities. The pressure coupling method described by Booker (2003) was used to calculate a free water surface elevation.

The utility of three-dimensional CFD (3D-CFD) applications can be enhanced by demonstrating the sensitivity of predictions to changes in the grid resolution (Hardy et al., 1999), treatment of turbulence closure (Lane, 1998) and flow resistance (Nicholas, 2001). For example, Booker (2003) demonstrated grid dependence experiments for CFD predictions for habitat assessments during high flows. These types

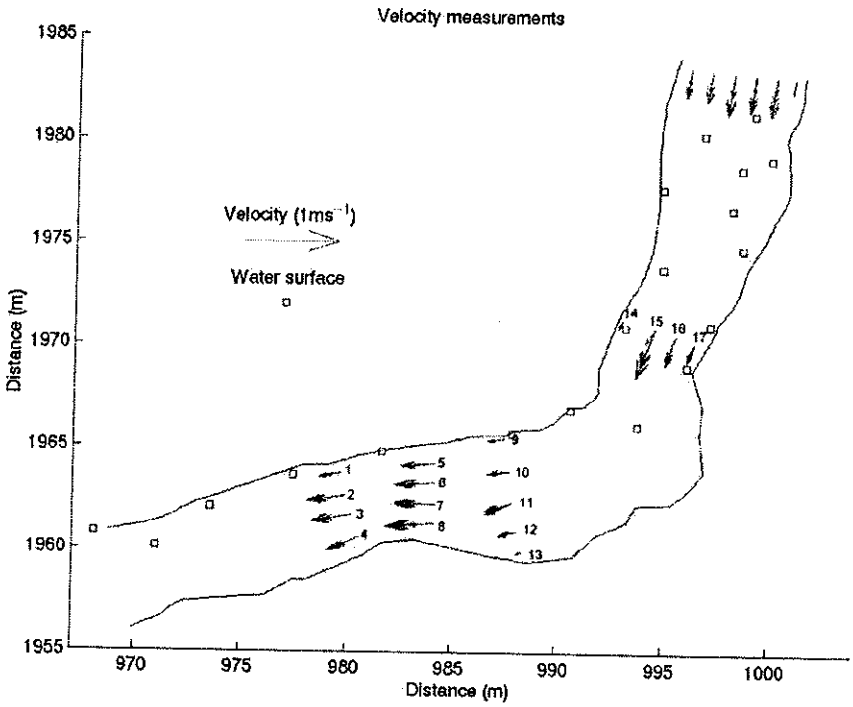

Fig. 3. The locations of the (ECM) velocity measurements at $0.52\,m^3\,s^{-1}$.

of assessments are not demonstrated in this paper; however, predicted water surface elevations and velocities were tested against field observations. Pairs of measured downstream water surface elevation and discharge were input to the model. Discharge was calculated in all cases using the velocity–area method (British Standard Institution, 1980). Water surface elevations throughout the reach were measured at flows of $0.45\,m^3\,s^{-1}$ (in July 2000), $1.01\,m^3\,s^{-1}$ (in February 2000) and $0.52\ m^3\,s^{-1}$ (in July 2001). Velocity profiles were measured at 23 locations across five cross-sections at the site at a flow of $0.52\,m^3\,s^{-1}$ during a 2-day period in July 2001 (Fig. 3). Data from the stage logger showed that water surface level did not change over this period. At each location velocity was measured at 0.05 m from the bed and every subsequent 0.05 m in the depth profile using a one-dimensional Valeport 801 electromagnetic current meter for a duration of 60 s. The position of each measurement was recorded using the total station. For each measurement the direction of flow was estimated with reference to the angle between a streamer attached to the current meter, and a tape measure stretched across the stream to the nearest 5°. Velocity was measured into the direction of flow. The locations of both ends of the tape were measured and triangulation used to find the direction of flow. One of these cross-sections was located at the upstream boundary of the model, whereas the other four cross-sections were distributed throughout the model domain (Fig. 3). Measurements at the upstream cross-section were taken to assess the level of variation in velocity across the inflow boundary.

2.3. Bioenergetic modelling methodology

Our bioenergetic model followed the conceptual framework set out by Hayes et al. (2000). This approach used a trade-off between energy gained through feeding and that lost through swimming costs of holding position and capture of food, as well as that lost in digestion, faces and urine. The energy balance was modelled using

$$E_{net} = E_{gross} - C_{swim} - C_{capture} - E_{digestion} - E_{urine} - E_{faces} \quad (2)$$

(Hughes and Kelly, 1996). Table 3 shows symbols, units and a description of each model variable. Physiological relationships used in the model were:

$$R = \frac{12L_{\text{prey}}(1 - e^{-0.2L_{\text{fish}}})}{100} \quad (3)$$

(Hughes and Dill, 1990)

$$v_{\max} = \frac{36.23L_{\text{fish}}^{0.19}}{100} \quad (4)$$

(Jones et al., 1974)

$$L_{\text{prey max}} = 0.4515L_{\text{fish}} \quad (5)$$

(Wankowski, 1979)

$$L_{\text{prey min}} = 0.0115L_{\text{fish}} \quad (6)$$

(Wankowski, 1979)

$$W_{\text{fish}} = 10^{(-4.419+2.733(\log(L_{\text{fish}}))/\log(10))} \quad (7)$$

(Elliott, 1984)

$$W_{\text{prey}} = \frac{0.019L_{\text{prey}}^{2.46}}{1000} \quad (8)$$

(Smock, 1980)

$$E_{\text{prey}} = \frac{0.3818L_{\text{prey}}^{2.46}}{4.18} \quad (9)$$

(Smock, 1980; Cummins and Wuycheck, 1971)

$$C_{\text{capture}} = t_{\text{capture}}n_{\text{capture}}\left\{\frac{[(1.4905W_{\text{fish}}^{0.784}\,e^{0.068T}\,e^{0.0259-0.005T}v_{\max} \times 100)/24]4.1868}{3600}\right\} \quad (10)$$

(Elliott, 1976; Rand et al., 1993)

$$C_{\text{swim}} = [3600 - (t_{\text{capture}}n_{\text{capture}})]\left\{\frac{[(1.4905W_{\text{fish}}^{0.784}\,e^{0.068T}\,e^{0.0259-0.005T}v_{\text{fish}} \times 100)/24]4.1868}{3600}\right\} \quad (11)$$

(Elliott, 1976; Rand et al., 1993)

Calculation of the total number of prey the fish could eat in an hour varies with temperature, where

$$\text{if } (T \geq 3.8) \text{ and } (T \leq 6.6) \Rightarrow D_{\max} = 0.654W_{\text{fish}}^{0.762}\,e^{0.418T} \quad (12)$$

(Elliott, 1975)

$$\text{if } (T \geq 6.7) \text{ and } (T \leq 13.6) \Rightarrow D_{\max} = 3.384W_{\text{fish}}^{0.759}\,e^{0.171T} \quad (13)$$

(Elliott, 1975)

Table 3
Symbols, units and description of model variables

Symbol	Units	Description
E_{net}	J h^{-1}	Net energy input
E_{gross}	J h^{-1}	Gross energy input
C_{swim}	J h^{-1}	Swimming costs of holding position against the flow
C_{capture}	J h^{-1}	The swimming cost incurred to capture prey
$E_{\text{digestion}}$	J h^{-1}	Energy lost through digestion
E_{urine}	J h^{-1}	Energy lost though urine and
E_{faces}	J h^{-1}	Energy lost though faces
T	°C	Temperature
L_{fish}	cm	Fish length
L_{prey}	mm	Prey length
n_{density}		Number of prey in each cubic meter of water
H	m	Distance from the fish snout to the bed
t_{capture}	s	Capture and handling time
R	m	Reaction distance
v_{fish}	ms^{-1}	Fish nose velocity
$v_{\max}$	ms^{-1}	Maximum sustainable swimming speed
$L_{\text{prey max}}$	mm	Minimum prey length
$L_{\text{prey min}}$	mm	Maximum prey length
W_{fish}	g	Fish weight
W_{prey}	g	Prey weight
E_{prey}	J	Energy per individual
n_{capture}		Total number of prey caught
$D_{\max}$	g h^{-1}	Maximum digestion rate
$E_{\text{gross max}}$	J h^{-1}	Maximum hourly consumption

$$\text{if } (T \geq 13.7) \text{ and } (T \leq 18.1) \Rightarrow D_{\max} = 5.956 W_{\text{fish}}^{0.767} e^{0.126T} \quad (14)$$

(Elliott, 1975)

$$E_{\text{gross max}} = \frac{D_{\max} E_{\text{prey}}}{W_{\text{prey}}} \quad (15)$$

$$E_{\text{faces}} = E_{\text{gross}}(0.212 T^{-0.222} e^{0.631}) \quad (16)$$

(Elliott, 1976)

$$E_{\text{urine}} = E_{\text{gross}}(0.0259 T^{-0.58} e^{-0.299}) \quad (17)$$

(Elliott, 1976)

The model algorithms for capture costs and energy intake were calculated separately for each prey size (Table 1) and then totalled to calculate E_{net}. Locations where local velocity exceeded $v_{\max}$ were modelled as having zero E_{net}.

2.4. Sensitivity to capture area calculation method

Calculation of capture areas for bioenergetic modelling requires an estimate of velocity. Velocity measurements from the field (e.g. Hughes and Dill, 1990; Guensch et al., 2001) or flume (e.g. Metcalf et al., 1997), hypothetical derivation (e.g. Hayes et al., 2000) or predictions from two-dimensional hydraulic models (Hayes et al., 2003) may be used. As a result some model calculations have relied on at-a-point measurements whereas others have utilised the spatially continuous information provided by hydraulic modelling techniques. In this paper, we demonstrate differences in bioenegetic predictions resulting from the assumptions made in calculating the capture area. Three methods of calculating the capture area are compared.

For the first method a semi-circular capture area, A, was determined by calculating the maximum capture distance, M, using measurements of depth-averaged velocity, v_{depthav}, and

$$M = \sqrt{R^2 - \left(\frac{R \times v_{\text{depthav}}}{v_{\max}}\right)^2} \quad (18)$$

(Hughes and Dill, 1990)

where R_{dist} is the reaction distance and v_{depthav} is the depth-averaged velocity. Allowing calculation of a semi-circular capture area

$$A = \pi M^2 \quad (19)$$

The swimming cost of the fish holding position was calculated using a logarithmic law (Gordon et al., 1992) to gain a value for the near-bed velocity that the fish is experiencing. This approach assumes that the depth-averaged velocity at the focal point of the fish represents the average velocity in the capture area and that the logarithmic representation of velocity profiles is accurate. All of these assumptions may to some extent be invalid in natural streams (Lane et al., 1999). A flat river bed is also assumed (e.g. Hayes et al., 2000). The second method was the same as the first, but allows truncation of the capture area where it meets the bed, banks, surface or any combination of these (e.g. Hughes and Dill, 1990). The first and second methods could be applied using predictions from a two-dimensional hydraulic model or a detailed set of mean column velocity measurements. The third method utilised the three-dimensional information provided by the hydraulic model. It was assumed that a drift-feeding fish must face into the direction of velocity at the point where the fish is waiting. The locations at which the fish can feed (making the capture area) are then calculated in a plane that is perpendicular to the direction in which the fish is pointing. This is done by calculating the reaction distance that would be required to catch prey at every point in a grid, $R_{\text{distrequired}}$, spanning this plane and then comparing this to the actual reaction distance, using

$$R_{\text{distrequired}} = \left(\frac{d_i^2}{1 - (v_i^2 / v_{\max})}\right)^{0.5} \quad (20)$$

where d_i is the distance from the fish to any point, i, in the plane and v_i is the velocity at that location. The fish can feed at any location where $R_{\text{distrequired}}$ is less than R. This method accounts for spatial variations in velocity and therefore allows calculation of irregular capture areas. The discharge passing through the capture area is then calculated using the distributed velocities within the capture area. This method will be referred to as the RDrequired method.

3. Results

3.1. Hydraulic model testing results

Differences between observed and predicted water surfaces were small in comparison to measurement error for measuring water surface elevations in the field (approximately ±0.005 m) (Table 4). The difference between observed and predicted water surface elevations was less than 0.005 m for 21 of all 31 comparisons. The largest difference between observed and predicted was less than 0.01 m.

Table 4
Comparisons of observed and predicted water surface elevation at discharges of 0.45, 0.52 and 1.01 $m^3 s^{-1}$

Discharge ($m^3 s^{-1}$)	Number of measurement	Distance downstream (m)	Observed–predicted (m)
0.45	1	0.17	0.0026
	2	13.24	−0.0057
	3	27.53	0.0087
	4	38.50	0.0074
	5	48.26	0.0027
	6	50.00	0.0020
Average difference			0.003
0.52	1	2.09	0.0000
	2	4.53	−0.0027
	3	5.23	0.0001
	4	6.97	−0.0014
	5	7.32	−0.0036
	6	9.41	−0.0064
	7	11.50	−0.0069
	8	13.94	−0.0025
	9	15.33	−0.0054
	10	16.72	−0.0056
	11	20.56	−0.001
	12	23.34	−0.0055
	13	28.57	−0.0029
	14	34.84	−0.0043
	15	39.02	−0.0046
	16	43.55	0.0019
	17	47.39	0.0000
	18	50.00	0.0000
Average difference			−0.0028
1.01	1	1.05	−0.0002
	2	13.24	0.0097
	3	28.40	0.0003
	4	38.50	−0.0046
	5	43.73	0.0029
	6	48.78	0.0076
	7	50.00	0.0000
Average difference			0.0022

Observed and predicted maximum velocity at each profile, as well as the cross-stream component, was compared (Fig. 4). The form of predicted velocity profiles corresponded well with the observed. Near-bed measurements were particularly well replicated, although there were exceptions. A high degree of correspondence for predicted and observed velocity profiles, and in particular near-bed velocities is a test of the realism of the roughness values employed in the model. Fig. 5 shows a comparison of the measured and modelled velocity vectors for all velocity measurements not positioned at the upstream boundary. Results show that in general there was a high degree of correspondence between observed and predicted velocity as the regression line was close to a one-to-one fit. The linear regression of predicted (U_{cal}) and observed (U_{obs}) velocities,

$$U_{obs} = 1.004U_{cal} - 0.024 \quad (21)$$

had an r^2 of 0.69. This level of agreement corresponds well with published comparisons between CFD predictions and observed velocities (Nicholas and Sambrook Smith, 1999; Hodskinson and Ferguson, 1998; Lane et al., 1999).

3.2. Sensitivity to capture area calculation results

Fig. 6 shows results of predicted E_{net} using three different methods for determining the capture area. The figure shows that where the capture area is not truncated predicted E_{net} is increased by more than a factor of four. This is because using the simplest semi-circular capture area method all predicted capture areas are semi-circular in shape, even in relatively shallow areas of the river and near to the banks. When truncation is included all areas within 1–0.5 m of the banks, and very shallow parts of the river, have E_{net} values that are reduced. The highest area of E_{net} is in the deepest part of the river, on the inside of the bend. However, E_{net} is relatively uniform throughout the middle of the river, particularly at the downstream end of the reach.

When the RDrequired method is used a contrasting map of E_{net} is predicted. The RDrequired method predicts that near-bank locations have higher E_{net} than the truncated semi-circular method. This is because

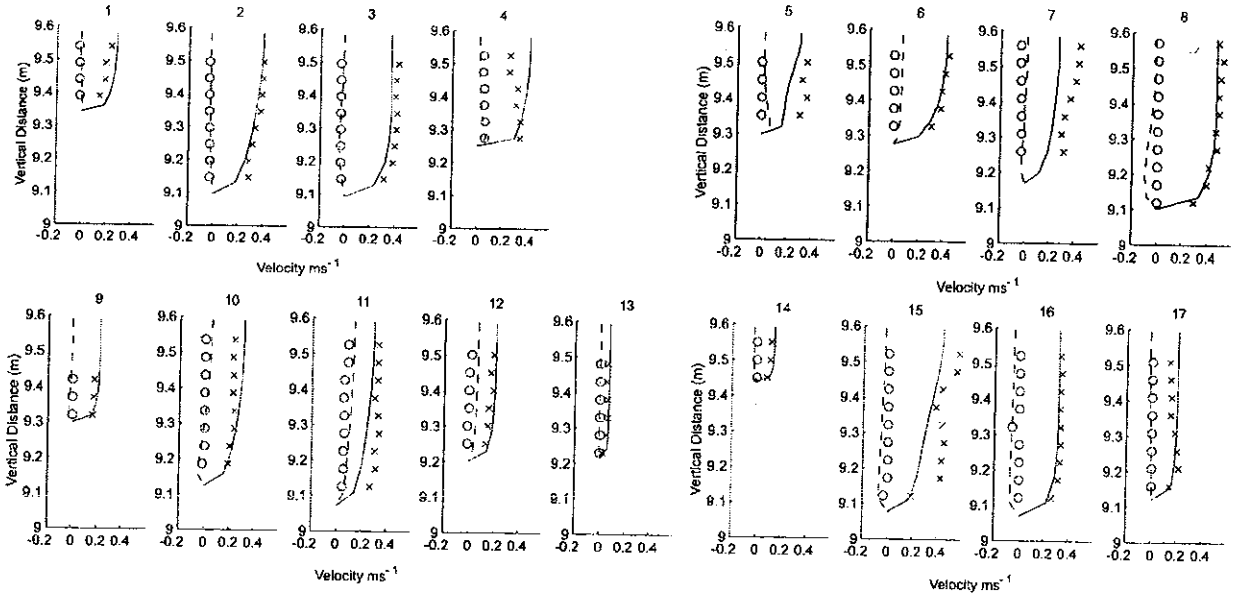

Fig. 4. Observed and predicted velocity profiles measured during a $0.52\,m^3\,s^{-1}$ flow at locations 1–17 shown in Fig. 3. Lines indicate predict velocity (solid for maximum velocity and dashed for secondary flow). Symbols represent observed velocity (crosses for maximum velocity and circles for secondary flow).

the RDrequired method allows simulated fish to have lower swimming cost whilst still being able to feed in the more profitable faster flowing areas toward the middle of the channel. Cross-stream gradients in E_{net} at some locations are also reduced for the same reason. This is reflected in cumulative frequency curves of E_{net} calculated using these two methods (Fig. 7). So, even though the RDrequired method gives a finer resolution of spatial variation, there are more locations within the model that have similar values of E_{net}.

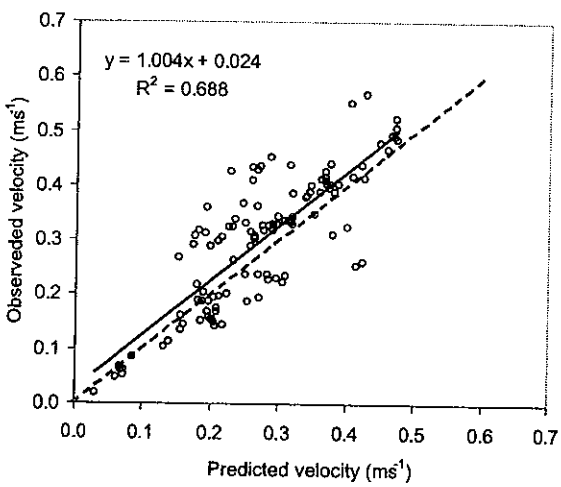

Fig. 5. A comparison of the observed and predicted velocity measurements at a flow of $0.52\,m^3\,s^{-1}$ ($n = 113$). Dashed line is $x = y$. Solid line is best fit to data.

E_{net} is relatively high in the downstream end of the reach. This is because this area has a relatively uniform bed shape causing the least lateral gradients in velocity. High E_{net} is predicted here because the cross-sectional area is smaller, producing higher velocities and a higher rate of prey delivery, and capture areas are truncated less in the deeper water.

3.3. Comparing predicted E_{net} with observed fish locations

The bioenergetic model was run for each occasion on which fish were observed, using the RDrequired method, input from the hydraulic model for a discharge of $0.4\,m^3\,s^{-1}$, measured drift densities and measured temperature. For the entire model domain, E_{net} was predicted for $L_{fish} = 0.1$ and 0.2 m at both high and low drift densities (Fig. 8). Results show that E_{net} did change with L_{fish} but that the spatial pattern of E_{net} was very similar. This means that the areas of highest E_{net} for the 0.1 m fish were the same as those

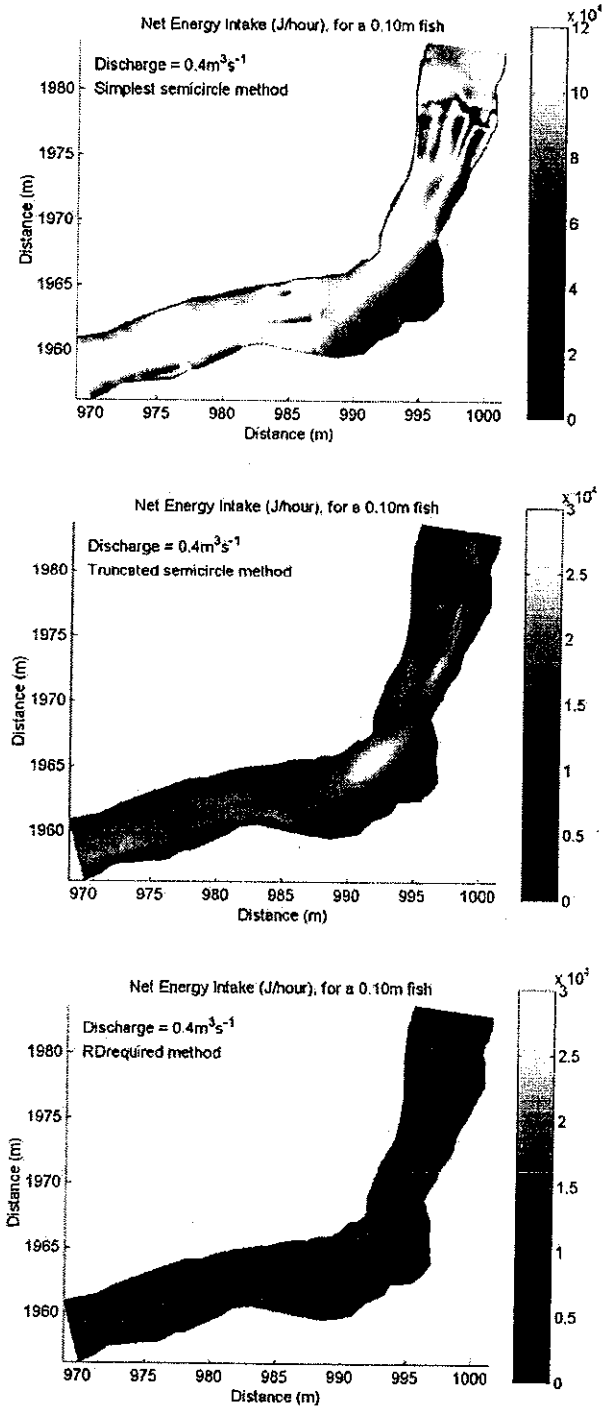

Fig. 6. Predicted E_{net} for different capture area calculation methods. Top: simplest semi-circular, middle: semi-circular, truncated, bottom: RDrequired. Discharge = $0.4\,m^3\,s^{-1}$, $H = 0.04\,m$, $L_{fish} = 0.1\,m$, average $n_{density}$ (Neale, 1999). Flow is from top to bottom.

for the 0.2 m fish at both drift densities. The model predicted that some locations with faster velocity could be occupied by 0.2 m fish but not by 0.1 m fish due to their slower swimming speeds. However, these were very shallow locations that had relatively low predicted E_{net} for the 0.2 m fish. Alternatively, for the lower drift density simulation some areas were less energetically profitable for the larger fish because their swimming costs were disproportionately costly in comparison with the smaller fish.

Given that the spatial pattern of E_{net} did not change significantly with L_{fish}, observed fish locations for all fish sizes on each occasion were compared with the predicted pattern of E_{net} for a 0.1 m fish (Fig. 9). Visual inspection of Fig. 9 suggests that fish were often found in or near to areas of generally higher E_{net}.

The following hypotheses were tested on predictions for 0.1 m fish for the six occasions on which fish were observed.

Hypothesis 1. All observed fish preferred areas of the stream with higher E_{net} (or v_{fish}) (tested by comparing E_{net} (or v_{fish}) at observed fish locations and predicted E_{net} (or v_{fish}) for the entire model domain).

Hypothesis 2. Same as for Hypothesis 1 but using feeding fish only.

Hypothesis 3. Feeding fish preferred areas of higher E_{net} (or v_{fish}) than resting fish (tested by comparing E_{net} at locations of feeding and resting fish).

Hypothesis 4. Resting fish avoid areas of higher v_{fish} (data as for Hypothesis 1 but using resting fish only).

Habitat preference indices (Fig. 10) were used to test Hypotheses 1, 2 and 4 for predicted E_{net} (or v_{fish}) and were calculated using the method of Jacobs (1974):

$$D_i = \frac{r_i - p_i}{r_i + p_i - 2r_i p_i} \tag{22}$$

where D is the calculated preference in class i, r is the proportion of habitat used in class i and p is the proportion of habitat available in class i. Positive indices indicate selective use of that habitat class and negative values indicate avoidance of that habitat class. Five

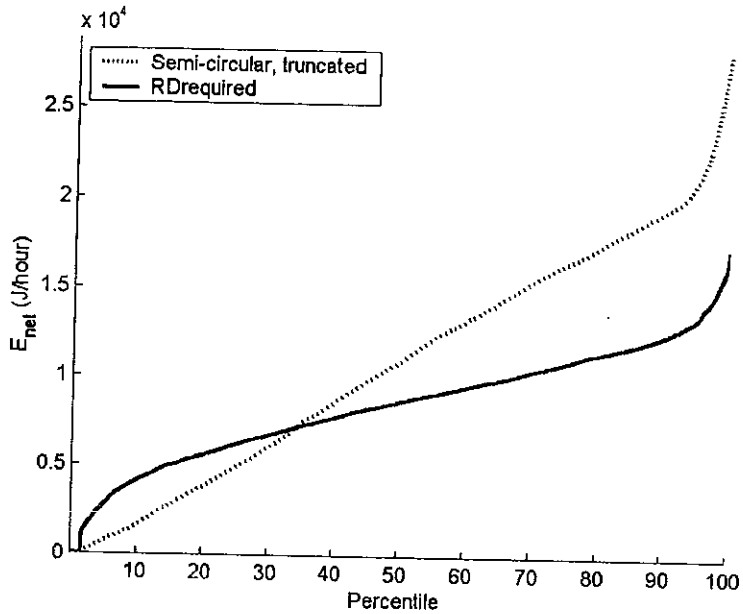

Fig. 7. Cumulative frequency of predicted E_{net} for different capture area calculation methods.

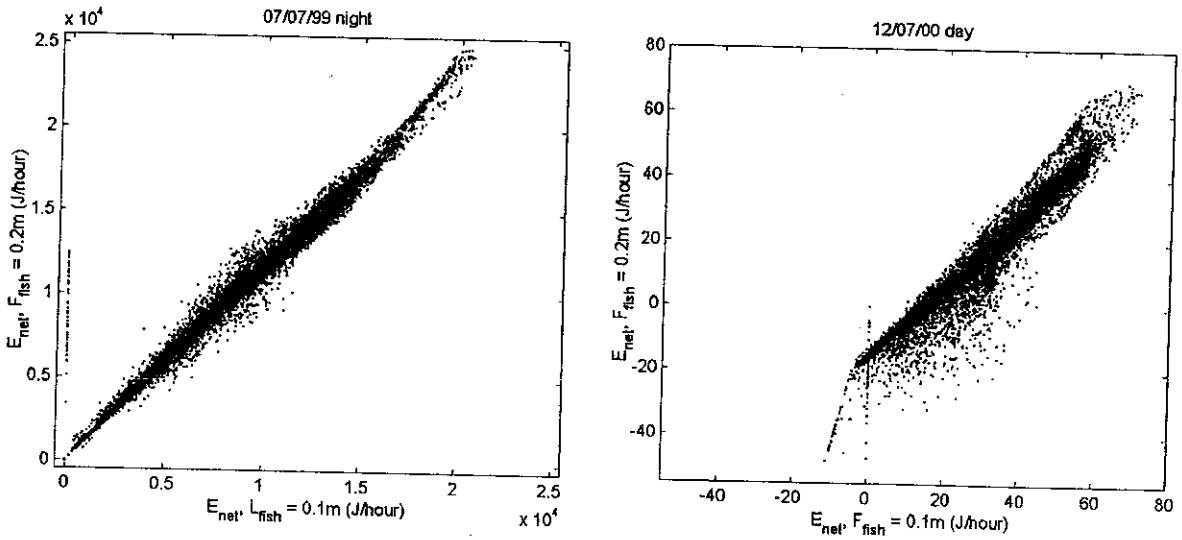

Fig. 8. Comparison of predicted E_{net} for 0.1 and 0.2 m F_L for 07/07/99 night (high drift density) and 12/07/00 day (low drift density) (n = 12,096).

classes of equal width were used, although the conclusions did not change if either four or six classes were chosen. Hypotheses 1–4 were also tested by comparing the mean or median values of predicted E_{net} (or v_{fish}) using t-tests/ANOVA and the nonparametric Wilcoxon/Mann–Whitney test (Hollander and Wolfe, 1973). Boxplots of the data are shown in Fig. 11.

3.4. Interpretation of calculated preference and statistical tests

There is considerable evidence that the observed fish locations were also areas of relatively high predicted E_{net} (Table 5). This supports Hypothesis 1. Visual inspection of the preference graphs supports

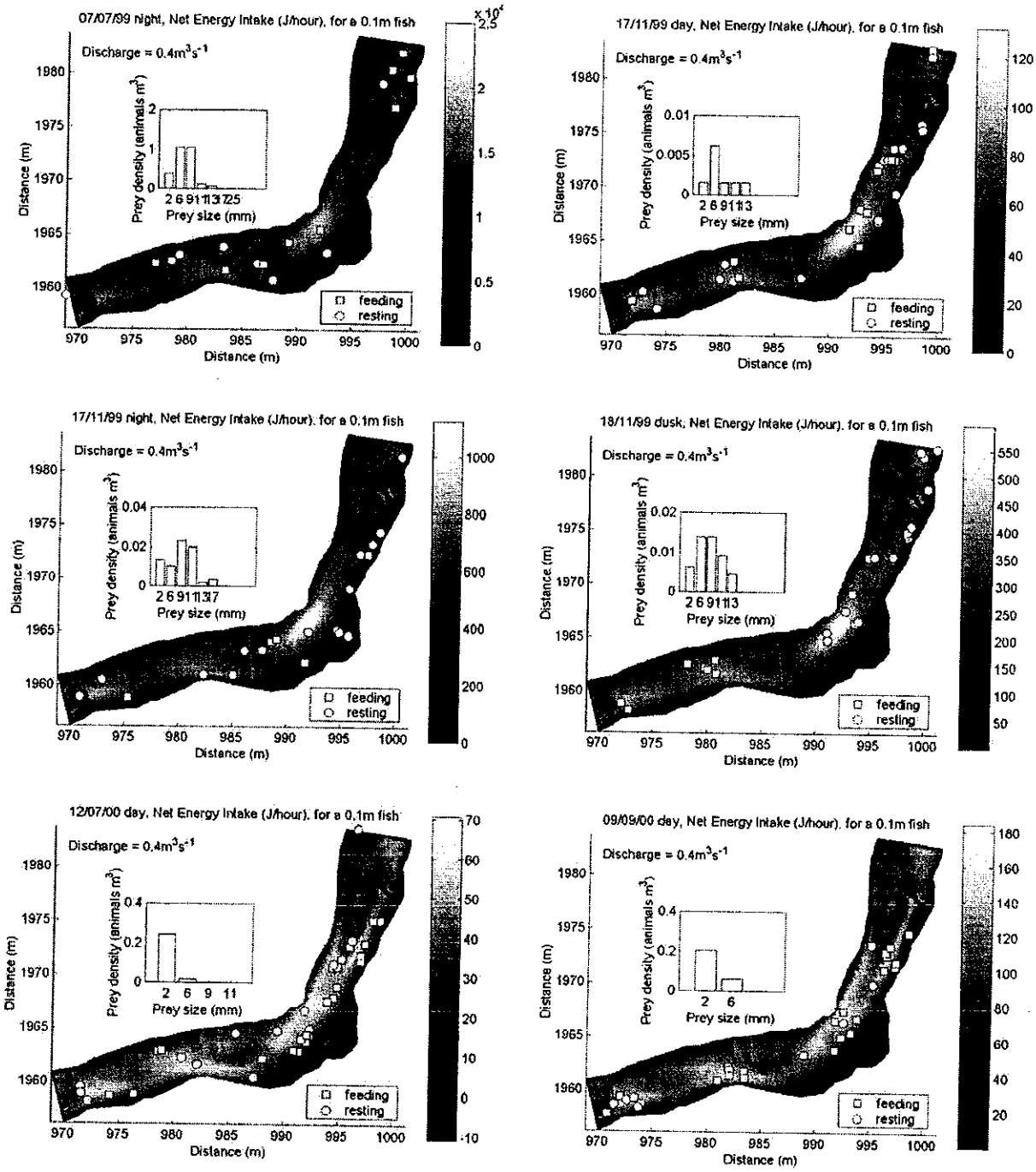

Fig. 9. Predicted E_{net} for a 0.1 m fish observed and fish locations for six occasions.

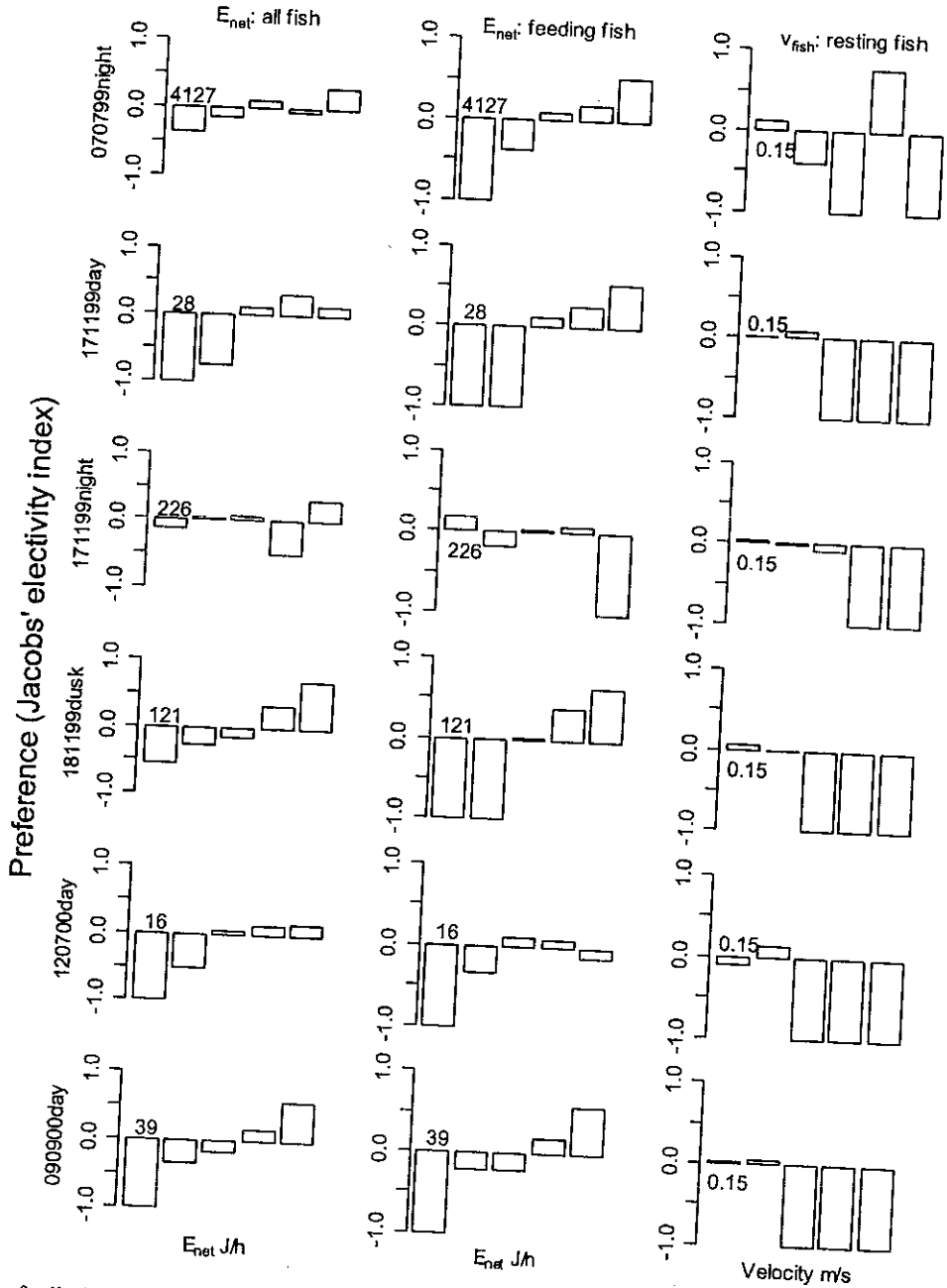

Fig. 10. Preference of: all observed fish for predicted E_{net} (left column); feeding fish for predicted E_{net} (middle column); and resting fish for predicted v_{fish} (right column) on each occasion. y-axis denotes preference where 1 indicates selection and −1 indicates avoidance. x-axis is divided into five equal categories the width of which (in units of $J\,h^{-1}$ or $m\,s^{-1}$) is indicated on each graph.

this on five out of six occasions, and the statistical tests support this on four out of six occasions. The exceptions were Occasion 3 from the preference graphs and Occasions 1 and 3 from the statistical tests. These were night surveys with the highest overall drift densities.

There is evidence to support Hypothesis 2 on four out of six occasions from the preference graphs, and

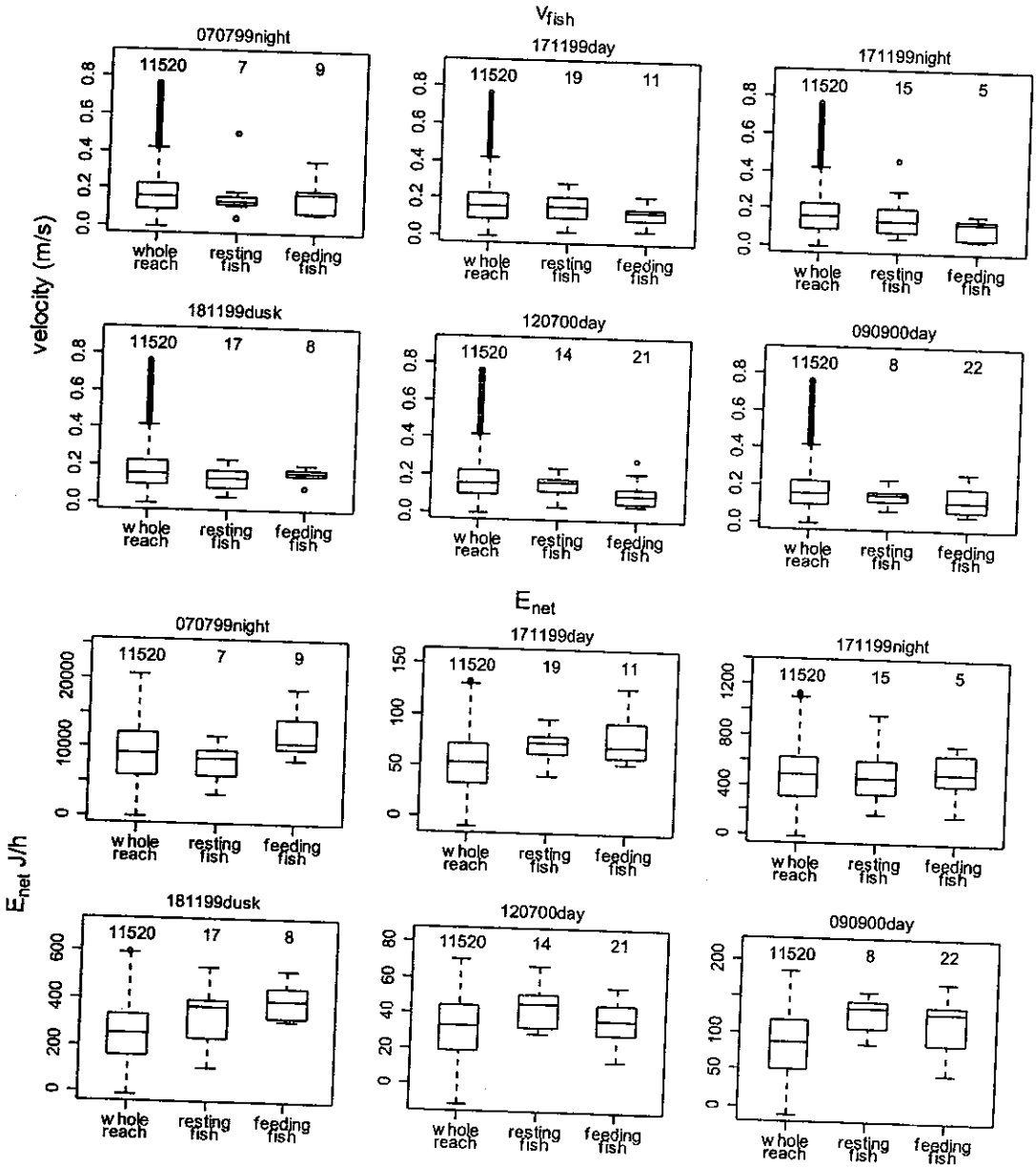

Fig. 11. Boxplots for each occasion of predicted E_{net} and v_{fish} for the whole reach, for observed resting fish, and for observed feeding fish. Numbers above boxes refer to sample sizes in each category.

four out of six occasions from the statistical tests. The exceptions were Occasions 3 and 5 from both the preference graphs and the statistical tests. Occasion 5 had the lowest drift density which consisted of relatively small prey. There is no evidence to support Hypothesis 3 on any occasion.

Figs. 10 and 11 show results for v_{fish} in addition to those for E_{net}. There is strong evidence to support Hypothesis 4 on all occasions using both visual inspection of the preference data and the statistical tests. For predicted v_{fish}, the first three hypotheses were supported only on Occasion 5, suggesting that E_{net} is a

Table 5
Results from preference calculations and statistical tests

	Occasion 1, 07/07/1999, night	Occasion 2, 17/11/1999, day	Occasion 3, 17/11/1999, night	Occasion 4, 18/11/1999, day	Occasion 5, 12/07/2000, day	Occasion 6, 09/09/2000, day
Interpretation of mapped E_{net} (Fig. 9)						
Hypothesis 1 E_{net}	Y	Y	N	Y	Y	Y
Hypothesis 2 E_{net}	Y	Y	N	Y	N	Y
Hypothesis 3 E_{net}	N	N	N	N	N	N
Interpretation of preference calculation (Fig. 10)						
Hypothesis 1 E_{net}	Y	Y	U	Y	Y	Y
Hypothesis 2 E_{net}	Y	Y	N	Y	U	Y
Hypothesis 4 v_{fish}	U	Y	Y	Y	Y	Y
Wilcoxon/Mann–Whitney test						
Hypothesis 1 E_{net}	0.30	0	0.99	0	0.0068	0
Hypothesis 2 E_{net}	0.033	0.0045	0.84	0	0.26	0
Hypothesis 3 E_{net}	0.34	0.89	0.88	0.17	0.99	0.82
Hypothesis 1 v_{fish}	0.73	0.29	0.21	0.26	0.015	0.062
Hypothesis 2 v_{fish}	0.95	0.17	0.14	0.9	0.0032	0.058
Hypothesis 3 v_{fish}	0.68	0.24	0.27	0.35	0.023	0.37
Hypothesis 4 v_{fish}	0	0	0	0	0	0

Y indicates hypothesis supported. N indicates hypothesis not supported. U indicates inconclusive results. Numbers indicate significance level of test. Zeros indicate values less than 10^{-4}.

more useful predictor of habitat quality than v_{fish}. The results indicate that resting fish were selecting areas of low velocity, but not necessarily areas of low E_{net}. All fish generally associated with high E_{net} except when E_{net} was very high overall. This could be because when energy as drift food is high everywhere in the reach, there is less need for fish to select the most profitable locations.

Feeding fish were associated with areas of high E_{net} except where E_{net} was very low overall. This could be because predicted E_{net} does not reflect true E_{net} at low drift densities. Drift density may be more spatially variable and driven in part by hydraulic and ecological processes that are not explicitly modelled here; for example, proximity to areas of invertebrate entrainment (Elliott, 1970; Anderwald et al., 1991; Stark et al., 2002).

4. Discussion

We have demonstrated that knowledge of the processes controlling hydraulics and physiology can be combined in order to produce testable, physically based habitat predictions. Feeding and resting salmonids selected areas of high bioenergetic profitability and resting fish selected areas of low velocity. However, this work has also shown that verification of drift-feeding bioenergetic models is difficult. This is because model calculations predict the energetic benefit of maintaining a certain position in the river for drift feeding. This is being compared with the actual locations of the fish in the river. This is not a true test of the accuracy of the model because factors other than energy intake can influence microhabitat selection. For example, the proximity to other fish (Valdimarsson and Metcalfe, 2001) and predation risk or distance to cover (Mesick, 1988). The fish do not spent 100% their time drift-feeding. They may feed very efficiently for short periods of time and then retreat to more sheltered locations (Gries and Juanes, 1998). Furthermore, the decision to select a certain position may not result from conditions (e.g. drift density) at that time, but conditions at a previous time or conditions over a longer period of time. Also, a fish may not have perfect knowledge of its habitat. This means that fish feeding in an energetically poor area may not be aware that there are more favourable alternative positions elsewhere.

Reaction distance can be affected by turbidity (Barrett et al., 1992) because fish vision is restricted as turbidity increases. This was not a factor in com-

parison of E_{net} and fish locations here as all fish observations were made in clear water conditions. However, reaction distance can also be reduced under low light conditions. Hayes et al. (2000) stated that the profitability of drift-feeding may become marginal at night, because the reaction distance to small prey has an asymptotic relationship with light intensity rapidly declining at low levels (Vinyard and O'Brien, 1976; Robinson and Trash, 1979; Henderson and Northcote, 1985; Hughes and Dill, 1990; Vogel and Beauchamp, 1999), but this limitation may be offset by the higher drift densities and general activity of aquatic invertebrates at night (McLay, 1968; Elliott, 1970; Waters, 1972; Brittain and Eikeland, 1988). Metcalf et al. (1997) showed that below 0.1 lx (similar to a full moon with a clear sky) fish were more efficient at intercepting food in slower flowing water. Table 1 shows that light levels, in terms of solar radiation, did vary between the snorkelling occasions. Although these measurements are not directly comparable with those taken by Metcalf et al. (1997) they did show that variations in light may have been sufficient to cause reductions in R at low light levels. However, the effect of a reduction in R for any given L_{fish} would be similar to that of reducing L_{fish}. Fig. 8 shows that this would reduce the values of predicted E_{net} but not its spatial pattern. Therefore, comparisons of predicted E_{net} and observed fish locations during very low light levels, such as at night, are valid.

Spatially distributed predictions of drift-feeding habitat quality for juvenile salmonids using three-dimension hydraulic information coupled with bioenergetic models incorporate many advantages over alternative physical habitat models. Bioenergetic model predictions do not rely on empirical Habitat Suitability Indices (HSIs). Use of HSIs has been criticised in the past for relying on expert opinion or, their lack of ecological reality (e.g. Orth and Maughan, 1982; Gore and Nestler, 1988; Holm et al., 2001). A physically based bioenergetic model avoids these problems. Furthermore, models that include process representation provide greater explanatory capabilities. This is because the effects of changes in specific factors can be separated from other model variables. The major advantage of bioenergetic modelling is that it uses available energy to describe habitat quality rather than empirically derived functions; the latter are difficult to extrapolate and do not explain habitat use. The use of energy also allows validation against population levels or growth potential which has proved difficult with empirical habitat models (Mathur et al., 1985). This work has shown that activity (feeding or resting) influences habitat selection. This implies that favourable conditions for a range of activities is required, even for a single life stage. This contradicts with habitat assessments that use a single HSI for a life stage regardless of activity.

Given appropriate model testing, more confidence can be placed in physically based predictions of conditions outside the measured range in comparison to empirically based models. This is particularly beneficial where assessments of hypothetical scenarios are required, such as changes in flow regime. It is relatively easy to make predictions of E_{net} given predicted hydraulic patterns at different discharges and a fixed drift density (Fig. 12). However, further research is required before this type of bioenergetic approach can be applied for environmental flow setting (Hayes et al., 2003). This is because it is difficult to predict spatial patterns in drift-density and changes in drift-density with changes in discharge at different times of day and year without large field data sets (Elliott, 2002; Hayes et al., 2003). Environmental flow setting also requires meaningful interpretation of predictions over a range of flows. Simply knowing the pattern of available E_{net} does not allow identification of a minimum flow.

Results have shown that the resolution of spatial variation in drift-feeding habitat is relatively fine in both the cross-stream and streamwise directions. Large changes in habitat quality can occur over very small distances. This means that assessment tools operating at the meso-habitat scale may not be able to detect changes in habitat quality. For example, a cross-section-based investigation of physical habitat of the reach shown in Fig. 9 might contain four to five cross-sections, each set across the middle of a riffle, pool or glide. However, predicted E_{net} shows that small changes in the location of these cross-sections would play an important role in the final outcome of the investigation. Fig. 9 also shows that habitat quality varies continuously, not only in the cross-stream direction, but also in the streamwise direction. A spatially continuous model allows investigation of physical changes in channel morphology at a specific

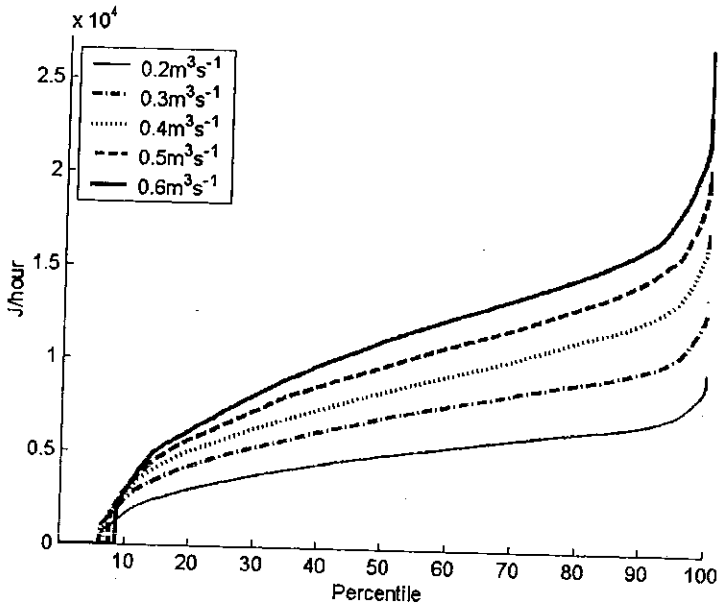

Fig. 12. Cumulative frequency of E_{net} using the average drift density (see Table 1) at different discharges.

location, for example, the impact of building a bridge or narrowing for river restoration.

Spatial representations of habitat quality may also assist in the development of IBMs (Grimm, 1999) for trout and salmon juveniles (Railsback and Harvey, 2002). For example, simulations of mortality rates and movement rules based on interactions between individuals may be sensitive to the spatial and temporal distribution of habitats (Railsback et al., 1999).

There are also disadvantages to employing bioenergetic models for physical habitat assessment and prediction. Bioenergetic models rely on the accuracy of various experiments and equations describing the physiological principles. Uncertainties within these equations will filter through to affect the final results. In addition, a large amount of field data and expertise are required to apply and test CFD models and the results produced often cover a relatively small area due to the requirement for high resolution field data to specify boundary conditions and the high computational demands of the model. Further work is required to investigate the utility of applying bioenergetic models linked to two- and three-dimensional hydraulic models in more complex channels (e.g. Waddle, 2000; Crowder and Diplas, 2000a) and whether these models can be upscaled to the catchment scale (Crowder and Diplas, 2000b; Crowder and Diplas, 2002).

5. Conclusion

This paper has described the use of a physically based three-dimensional bioenergetic model for drift-feeding salmonid habitat in a river. Modelled E_{net} was a good predictor of fish habitat use, except when drift density was high, and a good predictor of habitat used by feeding fish except when drift density was low. Nose velocity was not a useful predictor of habitat use by feeding fish, but resting fish did strongly select for low nose velocities. However, model testing is made difficult because behaviour of juvenile fish is affected by competition with other fish, cover from predation and imperfect knowledge of available habitat, as well as the energetic efficiency of available feeding locations.

Acknowledgements

Thanks to the many people who helped in collection of field data for this project: William Beaumont, Matthew Byrne, Sonja Folwell, Aurelie Malbrunot, Karen Thomas, Matthew Holmes, Jim Hudson, Abigail Ingram, Sadie Lees, Bethan Lewis, Neasa McDonnell, Martin Neale, Adrian Pinder and Nicole Weber. Particularly, thanks to Ian Gowing who organ-

ised much of the data collection, to Conor Linstead and Nicholas Naudin for initial model coding and fieldwork, to Nils Olsen for supplying the SSIIM code, to Thom Hardy and Craig Addley for fruitful discussions at the beginning of the project.

References

Acreman, M.C., Adams, B., Birchall, B., Connorton, B., 2000. Does groundwater abstraction cause degradation of rivers and wetlands. J. Chartered Inst. Water Environ. Manage. 14 (3), 200–206.

Anderwald, P.H., Konar, M., Humpesch, U.H., 1991. Continuous drift samples of macroinvertebrates in a large river, the Danube in Austria. Freshwater Biol. 25, 461–476.

Armstrong, J.D., Kemp, P., Kennedy, G., Ladle, M., Milner, N., 2003. Habitat requirements of Atlantic salmon and brown trout in rivers and streams. Fish. Res. 62 (2), 143–170.

Barrett, J.C., Grossman, G.D., Rosenfeld, J., 1992. Turbidity-induced changes in reactive distance of rainbow trout. Trans. Am. Fish. Soc. 121 (4), 437–443.

Beecher, H.A., Caldwell, B.A., DeMond, S.B., 2002. Evaluation of depth and velocity preferences of juvenile coho salmon in Washington streams. North Am. J. Fish. Manage. 22 (3), 785–795. AUG.

Bernard, R.S., 1993. STREMR: numerical model for depth averaged incompressible flow. Technical Report REMR-HY-11. US Army Corps of Engineers Waterways Experimental Research Station, Vicksburg, USA, 113 pp.

Binns, N.A., Eiserman, F.M., 1979. Quantification of Fluvial Trout Habitat in Wyoming. Trans. Am. Fish. Soc. 108 (3), 215–228.

Booker, D.J., 2003. Hydraulic modelling of fish habitat in urban rivers during high flows. Hydrol. Processes 17, 577–599.

Booker, D.J., Sear, D.A., Payne, A.J., 2001. Modelling three-dimensional flow structures and patterns of boundary shear stress in a natural pool-riffle sequence. Earth Surf. Processes Landforms 26, 553–576.

Bovee, K.D., 1982. A guide to stream habitat analysis using the IFIM. US Fish and Wildlife Service Report FWS/OBS-82/26, Fort Collins.

British Standard Institution, 1980. Methods of measurement of liquid in open channels, velocity area-methods. BS 3680, Part 3A. ISO 748-1979.

Brittain, J.E., Eikeland, T.J., 1988. Invertebrate drift—a review. Hydrobiologia 166, 77–93.

Clark, M.E., Rose, K.A., 1997. Individual-based model of stream-resident rainbow trout and brook char: model description, corroboration, and the effects of sympatry and spawning season duration. Ecol. Model. 94, 157–175.

Clifford, N.J., Robert, A., Richards, K.S., 1992. Estimation of flow resistance in gravel-bed rivers: a physical explanation of the multiplier of roughness length. Earth Surf. Processes Landforms 17, 111–126.

Crowder, D.W., Diplas, P., 2000a. Evaluating spatially explicit metrics of stream energy gradients using hydrodynamic model simulations. Can. J. Fish. Aquat. Sci. 57, 1497–1507.

Crowder, D.W., Diplas, P., 2000b. Using two-dimensional hydraulic models at scales of ecological importance. J. Hydrol. 230, 172–191.

Crowder, D.W., Diplas, P., 2002. Assessing changes in watershed flow models with spatially explicit hydraulic models. J. Am. Water Resour. Assoc. 38, 397–408.

Cummins, K.W., Wuycheck, J.C., 1971. Calorific equivalents for investigations in ecological energetics. Int. Vereinigung Theoret. Angewandte Limnol. 18, 1–158.

Elliott, C.R.N., Dunbar, M.J., Gowing, I.M., Acreman, M.C., 1999. A habitat assessment approach to the management of groundwater dominated rivers. Hydrol. Processes 13, 459–475.

Elliott, J.M., 1970. Methods of sampling invertebrate drift in running water. Ann. Limnol. 6 (2), 133–159.

Elliott, J.M., 1975. Number of meals in a day, maximum weight of food consumed in a day and maximum rate of feeding for brown trout, *Salmo trutta* L. Freshwater Biol. 45, 561–580.

Elliott, J.M., 1976. Energy losses in the waste products of brown trout (*Salmo trutta* L.). J. Anim. Ecol. 45, 561–580.

Elliott, J.M., 1984. Growth, size, biomass and production of young migratory trout *Salmo trutta* in a Lake District stream, 1966–83. J. Anim. Ecol. 53, 979–994.

Elliott, J.M., 2002. A continuous study of the total drift of freshwater shrimps, *Gammarus pulex*, in a small stony stream in the English Lake District. Freshwater Biol. 47, 75–86.

Fausch, K.D., 1984. Profitable stream for salmonids relating specific growth rate to net energy gain. Can. J. Zool. 62, 441–451.

Gordon, N.D., McMahon, T.A., Finlayson, B.L., 1992. Stream Hydrology: An Introduction for Ecologists. Wiley, Chichester, 526 pp.

Gore, J.A., Nestler, J.M., 1988. Instream flow studies in perspective. Regul. Rivers: Res. Manage. 2, 93–101.

Gries, G., Juanes, F., 1998. Microhabitat use by juvenile Atlantic salmon (*Salmo salar*) sheltering during the day in summer. Can. J. Zool. 76 (8), 1441–1449.

Grimm, V., 1999. Ten years of individually-based modelling in ecology: what have we learned and what could we learn in the future? Ecol. Model. 115, 129–148.

Guensch, G.R., Hardy, T.B., Addley, R.C., 2001. Examining feeding strategies and position choice of drift-feeding salmonids using an individual-based, mechanistic foraging model. Can. J. Fish. Aquat. Sci. 58, 446–457.

Harby, A., Alfredsen, K., 1998. Application of new modelling tools for spatial physical habitat assessments. In: Proceedings of VII Intecol Congress, July 19–25, Florence, Italy.

Hardy, R.J., Bates, P.D., Anderson, M.G., 1999. The importance of spatial resolution in hydraulic models for floodplain environments. J. Hydrol. 216, 124–136.

Hayes, J.W., Stark, J.D., Shearer, K.A., 2000. Development and test of a whole-lifetime foraging and bioenergetics growth model for drift feeding brown trout. Trans. Am. Fish. Soc. 125, 315–332.

Hayes, J.W., Hughes, N.F., Kelly, L.H., 2003. Overview of a process-based model relating stream discharge to the quantity and quality of brown trout habitat. In: Proceedings of the International IFIM Workshop, Fort Collins, Colorado, June 2003.

Heggenes, J., 1996. Habitat selection by brown trout (*Salmo trutta*) and young Atlantic salmon (*S. salar*) in streams: static and dynamic hydraulic modelling. Regul. Rivers: Res. Manage. 12, 155–169.

Heggenes, J., Saltveit, S.J., 1990. Seasonal and spatial microhabitat selection and segregation in young Atlantic salmon, *Salmo salar* L, and brown trout, *Salmo trutta* L., in a Norwegian river. J. Fish Biol. 36, 707–720.

Henderson, M.A., Northcote, T.G., 1985. Visual prey detection and foraging in sympatric cutthroat trout (*Salmo clarki clarki*) and Dolly Varden (*Salvelinus malma*). Can. J. Fish. Aquat. Sci. 42, 785–790.

Hey, R.D., 1986. River mechanics. Jnl. Inst. Water Eng. Scientists 40, 139–158.

Hill, J., Grossman, G.D., 1993. An energetic model of microhabitat use for rainbow-trout and rosyside dace. Ecology 74 (3), 685–698.

Hodskinson, A., Ferguson, R.I., 1998. Numerical modelling of separated flow in river bends: model testing and experimental investigation of geometric controls on the extent of flow separation at the concave bank. Hydrol. Processes 12, 1323–1338.

Hollander, M., Wolfe, D.A., 1973. Nonparametric Statistical Inference. New York, Wiley.

Holm, C.F., Armstrong, J.D., Gilvear, D.J., 2001. Investigating a major assumption of predictive instream habitat models: is water velocity preference of juvenile Atlantic salmon independent of discharge? J. Fish Biol. 59 (6), 1653–1666.

Hughes, N.F., 1992. Selection of positions by drift-feeding salmonids in dominance hierarchies: model and test for Arctic grayling (*Thymallus arcticus*) in subartic mountain streams, interior Alaska. Can. J. Fish. Aquat. Sci. 49, 1999–2008.

Hughes, N.F., Dill, L.M., 1990. Position choice by drift feeding salmoniods: model and test for Arctic Grayling (*Thymallus arcticus*), in subarctic mountain streams, interior Alaska. Can. J. Fish. Aquat. Sci. 47, 2039–2048.

Hughes, N.F., Kelly, L.K., 1996. A hydrodynamic model for estimating the energetic cost of swimming maneuvers from a description of their geometry and dynamics. Can. J. Fish. Aquat. Sci. 53, 2484–2493.

Jacobs, J., 1974. Quantitative measurement of food selection: a modification of the forage ratio and Ivlev's electivity index. Oecologia 14, 413–417.

Jones, D.R., Kiceniuk, J.W., Bamford, O.S., 1974. Evaluation of swimming performance of several fish species from the MacKenzie River. J. Fish. Res. Board Can. 31, 1641–1647.

Jungwirth, M., 1988. Rekultivierung von Fließgewässern. Die Varianz der Maximaltiefen als morphometrisches Kriterium. Wertermittlungsformum, Jhg 6 (3), 105–111.

Lane, S.N., 1998. Hydraulic modelling in geomorphology and hydrology: a review of high resolution approaches. Hydrol. Processes 12, 1131–1150.

Lane, S.N., Bradbrook, K.F., Richards, K.S., Biron, P.A., Roy, A.G., 1999. The application of computational fluid dynamics to natural river channels: three-dimensional versus two-dimensional approaches. Geomorphology 29, 1–20.

Leopold, L.B., Wolman, M.G., Miller, J.P., 1964. Fluvial Processes in Geomorphology. Freeman, San Francisco, 522 pp.

Lin, Y.M., Chen, C.N., Lee, T.H., 2003. The expression of gill Na, K-ATPase in milkfish, *Chanos chanos*, acclimated to seawater, brackish water and fresh water. Comp. Biochem. Physiol. Part A Mol. Integr. Physiol. 135, 489–497.

Maddock, I., 1999. The importance of physical habitat assessment for evaluating river health. Freshwater Biol. 41 (2), 373–391.

Mathur, D., Bason, W.H., Purdy, E.J., Silver, C.A., 1985. A critique of the instream flow incremental methodology. Can. J. Fish. Aquat. Sci. 42, 825–831.

McLay, C.L., 1968. A study of drift in the Kakanui River, New Zealand. Aust. J. Marine Freshwater Res. 19, 139–149.

Mesick, C.F., 1988. Effects of food and cover on numbers of apache and brown trout establishing residency in artificial stream channels. Trans. Am. Fish. Soc. 117, 421–431.

Metcalf, B.N., Valdimarsson, S.K., Fraser, N.H.C., 1997. Habitat profitability and choice in a sit-and-wait predator: juvenile salmon prefer slower currents on darker nights. J. Anim. Ecol. 66, 866–875.

Neale, M., 1999. An investigation of the spatial distribution of drifting invertebrates in a chalk stream. A dissertation submitted as part of the requirements for the degree of MSc/PGDip Environmental Quality, School of Conservation Sciences, Bournemouth University.

Nicholas, A.P., 2001. Computational fluid dynamics modelling of boundary roughness in gravel-bed rivers: an investigation of the effects of random variability in bed elevation. Earth Surf. Processes Landforms 26, 345–362.

Nicholas, A.P., Sambrook Smith, G.H., 1999. Numerical simulation of three-dimensional flow hydraulics in a braided river. Hydrol. Processes 13, 913–929.

Olsen, N.R.B., 1996. A three-dimensional numerical model for simulation of sediment movements in water intakes with multi-block option. In: SSIIM Users Manual Version 1.4.

Olsen, N.R.B., 2000. A three-dimensional numerical model for simulation of sediment movements in water intakes with multi-block option. In: SSIIM Users Manual Version 1.1 and 2.0 for OS/2 and Windows. 112 pp.

Olsen, N.R.B., Stokseth, S., 1995. Three-dimensional numerical modelling of water flow in a river with large bed roughness. IAHR J. Hydraulic Res. 33, 571–581.

Orth, D.J., Maughan, O.E., 1982. Evaluation of the incremental methodology for recommending instream flows for fishes. Trans. Am. Fish. Soc. 111, 413–445.

Parasiewicz, P., Dunbar, M.J., 2001. Physical habitat modelling for fish: a developing approach. Arch. Hydrobiol. Suppl. 135 (2–4), 1–30.

Railsback, S.F., Harvey, B.C., 2002. Analysis of habitat-selection rules using as individual-based model. Ecology 83, 1817–1830.

Railsback, S.F., Rose, K.A., 1999. Bioenergetics modelling of stream trout growth: temperature and food consumption. Trans. Am. Fish. Soc. 128, 241–256.

Railsback, S.F., Lamberson, R.H., Harvey, B.C., 1999. Movement rules for individual-based models of stream fish. Ecol. Model. 123, 73–89.

Rand, P.S., Stewart, D.J., Seelbach, P.W., Jones, M.L., Wedge, L.R., 1993. Modeling steelhead population energetics in lakes

Michigan and Ontario. Trans. Am. Fish. Soc. 122, 977–1001.

Robinson, F.W., Trash, J.C., 1979. Feeding by Arizona trout (*Salmo apache*) and brown trout (*Salmo trutta*) at different light intensities. Environ. Biol. Fishes 4, 363–368.

Scheibe, T.D., Richmond, M.C., 2002. Fish individual-based numerical simulator (FINS): a particle based model of juvenile salmonid movement and dissolved gas exposure history in the Columbia River basin. Ecol. Model. 147, 233–252.

Shirvell, C.S., Dungey, R.G., 1983. Microhabitats chosen by brown trout for feeding and spawning in rivers. Trans. Am. Fish. Soc. 112, 355–367.

Smock, L.A., 1980. Relationships between body size and biomass of aquatic insects. Freshwater Biol. 10, 375–383.

Soulsby, C., Youngson, A.F., Moir, H.J., Malcolm, I.A., 2001. Fine sediment influence on salmonid spawning habitat in a lowland agricultural stream: a preliminary assessment. Sci. Total Environ. 265 (1–3), 295–307.

Stark, J.D., Shearer, K.A., Hayes, J.W., 2002. Are aquatic invertebrate drift-densities uniform? Implications for salmonid foraging models. Verhandlungen Int. Vereinigung Theoret. Angewandte Limnol. 28, 988–991.

Valdimarsson, S.K., Metcalfe, N.B., 2001. Is the level of aggression and dispersion in territorial fish dependent on light intensity? Anim. Behav. 61, 1143–1149.

Vinyard, G.L., O'Brien, W.J., 1976. Effects of light and turbidity on the reactive distance bluegill (*Lepomis macrochirus*). J. Fish. Res. Board Can. 33, 2845–2849.

Vogel, J.L., Beauchamp, D.A., 1999. Effects of light, prey size, and turbidity on reaction distances of lake trout (*Salvelinus namaycush*) to salmonid prey. Can. J. Fish. Aquat. Sci. 56 (7), 1293–1297.

Volpe, J.P., Glickman, B.W., Anholt, B.R., 2001. Reproduction of aquaculture Atlantic salmon in a controlled stream channel on Vancouver Island, British Columbia. Trans. Am. Fish. Soc. 130 (3), 489–494.

Waddle, T., et al., 2000. Comparison one and two dimensional open channel flow models for a small habitat stream. Rivers 7 (3), 205–220.

Wankowski, J.W.J., 1979. Morphological limitations, prey size selectivity, and growth response of juvenile Atlantic salmon, *Salmo salar*. J. Fish Biol. 14, 89–100.

Waters, T.F., 1972. The drift of stream insects. Ann. Rev. Entomol. 17, 253–272.